Solvability condition for the moving contact line

L. M. Pismen[1] and Jens Eggers[2]

[1]*Department of Chemical Engineering and Minerva Center for Nonlinear Physics of Complex Systems,*
Technion–Israel Institute of Technology, Haifa 32000, Israel
[2]*School of Mathematics, University of Bristol, University Walk, Bristol BS8 1TW, United Kingdom*

We consider the motion of a contact line between a fluid, gas, and solid, as it occurs when a drop advances over a solid surface. This motion is controlled by a microscopic length scale near the contact line, such as a slip length or the precursor thickness. The capillary profile inside the drop is linked to the contact line through an intermediate region which is characterized by an interface slope which varies logarithmically. The intermediate solution contains a single adjustable constant, which can be computed either by matching to the capillary region or to the contact line. We describe a simple method to perform the matching and to compute the required constant. This extends and/or simplifies results known previously. We apply our results to the case of a spreading drop in the presence of an interface potential and derive the equation of motion by combining the inner and outer expansions.

I. INTRODUCTION

The moving contact line problem remains the focus of wide theoretical interest, in view of both its practical importance and a great variety of physical factors operating on nanoscale but influencing both macroscopic motion and interfacial shape far from the contact line (see [1–3] for recent reviews). Both analytical and numerical studies are commonly based on the lubrication approximation, leading to the evolution equation of the film thickness $h(t, \mathbf{x})$ in time t:

$$h_t = -\boldsymbol{\nabla}\{q(h)\,\boldsymbol{\nabla}\,[\,\gamma\nabla^2 h - \Pi(h) - W(h,\mathbf{x})]\}. \tag{1}$$

Here $q(h)$ is the mobility function equal to $\frac{1}{3}h^3/\eta$ in a standard case of Stokes flow with the viscosity η and no slip; $\boldsymbol{\nabla}$ is the gradient operator in the $\mathbf{x}$ plane, γ is the surface tension, $\Pi(h)$ is the disjoining pressure, and $W(h,\mathbf{x})$ is some (space dependent) external potential, e.g., the gravitational potential on an inclined plane.

In most contact line problems of practical importance, there exists an outer region, away from the contact line, where viscous forces are not important, and the shape of the interface is determined by capillarity in conjunction with external potentials, such as gravity, or volume constraints. The contact line itself, on the other hand, is characterized by a microscopic length scale, on the order of a few nm at most. In this inner region intermolecular forces are important, apart from viscous forces, and other physical factors, like slip and diffuse interface effects. Numerical computations of shapes of moving menisci and spreading droplets are technically difficult even in the lubrication approximation of Eq. (1), in view of a vast disparity between the macroscopic and microscopic scales. Analytical theory exploits this separation by applying multiscale expansion and matching techniques applicable at low velocities.

Voinov [4] was the first to observe that there exists an intermediate region, which connects the inner and outer regions, where only viscous and surface tension forces are important. The dynamics of this region is controlled by the capillary number $\mathrm{Ca} = U\eta/\gamma$, where U is the contact line speed (assumed to be positive when the contact line advances). In the intermediate region, the interface slope is of the form

$$[h'(x)]^3 = \theta^3 + 9\mathrm{Ca}\,\ln(x/x_0), \tag{2}$$

where θ is an asymptotic angle and x is the distance from the contact line. The latter implies that Eq. (2) is formulated in the frame of reference of the contact line. The crucial feature of the Voinov solution is that the prefactor in front of the logarithm is universal, independent of any other parameter of the inner or outer solutions. On the other hand, the characteristic length x_0 remains indefinite, if only viscous and surface tension forces are taken into account. To calculate x_0, Eq. (2) needs to be matched to either the contact line itself, or to the macroscopic profile away from the contact line. Since the result for x_0 must be the same in both cases, Eq. (2) provides the missing link between the macroscopic interface profile and the microscopic features of the contact line. The angle θ can be formally incorporated into x_0, but it is retained since it can be further specified in a way suitable for the matching procedure.

Matching Eq. (2) analytically to the meniscus on an inclined plane or to a spherical cap solution that makes up the bulk of the spreading drop becomes possible to first order of the expansion in $\mathrm{Ca} \ll 1$, since the *curvature* vanishes for $x \to \infty$. Analytical matching has been carried out in [5,6] for the case when fluid slip over the solid surface relieves the contact line singularity. Here we adopt a model that builds in the equilibrium properties in a more rational way, by including the interface potential into the description. Both the equilibrium contact angle [7] and the equilibrium film thickness h_f are determined by the interface potential. Within the model, even the "dry" substrate is covered by a thin film, corresponding to the minimum of the interface potential [8,9]. The presence of this film thus formally eliminates the contact line singularity, h_f playing the role of a microscopic length scale. Of course, we do not claim that this is a universal resolution of the contact line problem. The thickness h_f is sometimes below the thickness of a single molecule,
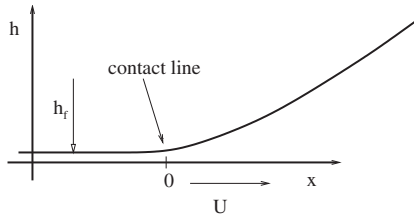
FIG. 1. A cartoon of the contact line. In a frame of reference in which the contact line position is stationary, the solid moves to the right with velocity U. There is a very thin film of thickness h_f in front of the contact line.

and even a monomolecular layer is not strictly describable by a continuum theory (see Fig. 1).

Expansion and matching involving disjoining potential in partially wetting fluids is more difficult, because of coordinate-dependent terms in the first-order equation stemming from the function $\Pi(h)$. Recently, one of us [10] solved this problem using a particular function $\Pi(h)$ for which an analytical solution happened to be available. A more economical method based on computing the solvability condition of the first-order equation and dispensing with the need to actually solve this equation was applied [11,12] to computing velocity of moving droplets (in situations when dynamic reshaping of droplets is not important).

In this paper, we extend the method to treatment of moving menisci and spreading droplets where, unlike [11,12], dynamic interface reshaping is essential. The paper is organized as follows. In Sec. II, we recall the case of a static contact line, relating the equilibrium contact angle to the interface potential, and outline how a free scaling parameter of the intermediate solution can be found by computing the solvability condition of the expansion in the inner region. The same parameter can be alternatively computed through a solvability condition of the expansion in the outer region. In Sec. III, this procedure is carried out explicitly for a spreading droplet, and the macroscopic equation of motion is obtained by matching the two expansions in Sec. IV.

II. MATCHING TO THE PRECURSOR FILM

We consider a contact line region, of microscopic size, in the presence of a disjoining potential and neglecting the effect of slip or of finite interface width. In the case of a partially wetting fluid, a microscopically thin film covering the substrate in front of the contact line is in equilibrium with a flat bulk fluid interface. The thickness of this film h_f defined by a particular form of the disjoining pressure $\Pi(h)$ [8,9] serves as the microscale resolving the contact line singularity.

On the microscopic scale, the contact line can effectively be considered as being straight, so the problem reduces to a one-dimensional equation. Assuming the motion to be quasistationary and using h_f as the length scale, we set

$$h(x) = h_f H(\xi), \quad \xi = x\theta_0/h_f, \tag{3}$$

where θ_0 is the equilibrium contact angle. As before, x is the distance to the contact line, so that the problem is formulated

in the frame of reference of the contact line, which advances at speed U. Using this ansatz in Eq. (1) with the mobility $q(h) = \frac{1}{3}h^3/\eta$ gives, after one integration,

$$\frac{\delta(H-1)}{H^3} + [H_{\xi\xi} - f(H)]_\xi = 0, \tag{4}$$

where $f(H) = h_f \Pi(h)/(\gamma\theta_0^2)$ is the dimensionless disjoining pressure and the rescaled capillary number δ is

$$\delta = \frac{3\text{Ca}}{\theta_0^3} = \frac{3\eta U}{\gamma\theta_0^3}. \tag{5}$$

The rescaled capillary number δ, which is a combination of speed and a typical interface angle, is the natural expansion parameter of the problem. One should keep in mind that it is a combination of the form (5) that has to be small for the present lubrication approach to be valid.

Suitable functions $f(H)$ have the form

$$f(H) = \frac{n-1}{n-3}\left(\frac{1}{H^3} - \frac{1}{H^n}\right). \tag{6}$$

The first term in the parentheses is Derjaguine's [13] classical disjoining pressure stemming from van der Waals interactions; the sign corresponds to weak attraction between the free interface and the substrate characteristic to partially wetting fluids where fluid-fluid attraction forces at equilibrium liquid density are stronger than fluid-substrate interactions. The second term, having the opposite sign, keeps the film thickness from collapsing to zero. A popular choice, $n=9$, which is motivated by the form of the repulsive Lennard-Jones interaction, stems from a misunderstanding, since repulsive intermolecular interactions cause, on the contrary, attraction between the free interface and the substrate. The value $n=6$ derived in the long-scale limit starting from the nonlocal diffuse interface theory with usual van der Waals interactions [9] is the best physically motivated choice for layers thick compared to a molecular scale. For thinner layers, different powers may follow from different molecular interaction models [14]. Recently, considerable progress has been made in determining the form of $\Pi(h)$ for some systems [15]. However, the experiments are still not sufficiently accurate to uniquely determine the value of the exponent n [16].

For $\xi \to -\infty$, the solution of Eq. (4) tends toward the equilibrium precursor film: $H(-\infty) = 1$. On the other side, for $\xi \to \infty$, it reaches the Voinov solution (2). We perform the calculation in a perturbation expansion in δ:

$$H(\xi) = H_0(\xi) + \delta H_1(\xi) + O(\delta^2). \tag{7}$$

To zeroth order, the static profile near the contact line is computed. It is convenient to use a "phase plane" representation obtained by taking the layer thickness H_0 as the independent variable, and the squared slope $y = [H_0'(\xi)]^2$ as the dependent variable:

$$y'(H_0) = 2f(H_0), \quad y(1) = 0. \tag{8}$$

Using Eq. (6), this can be integrated to

$$y = 1 - \frac{n-1}{n-3}\frac{1}{H_0^2} + \frac{2}{n-3}\frac{1}{H_0^{n-1}}. \qquad (9)$$

The asymptotic equilibrium contact angle $H_0'(\infty) = \sqrt{y(\infty)}$ is normalized to unity.

The equation for H_1 can be written in the form

$$\mathcal{L}H_1 + \Psi(\xi) = 0, \qquad (10)$$

containing a linear operator

$$\mathcal{L} = \partial_\xi[\partial_\xi^2 - f'(H_0)] \qquad (11)$$

and an inhomogeneity

$$\Psi(x) = \frac{H_0(\xi)-1}{H_0^3}. \qquad (12)$$

Due to the translational invariance, Eq. (10) and its adjoint

$$\mathcal{L}^\dagger = -[\partial_\xi^2 - f'(H_0)]\partial_\xi \qquad (13)$$

have a zero eigenvalue. The corresponding eigenfunction φ that lies in the kernel of $\mathcal{L}^\dagger$ and vanishes at $\xi \rightarrow -\infty$ is $\varphi = H_0 - 1$.

The solvability condition of Eq. (10) is obtained by multiplying it by φ, and integrating over a domain large when measured on the inner scale but small when measured on the outer scale, so that the intermediate solution (2) holds on its boundary $\xi = \ell$:

$$\int_{-\infty}^{\ell} \varphi \mathcal{L}H_1 d\xi + \int_{-\infty}^{\ell} \varphi \Psi d\xi = 0. \qquad (14)$$

Since $\mathcal{L}^\dagger \varphi = 0$, the first integral can be reduced to boundary terms; after three partial integrations, one is left with

$$\int_{-\infty}^{\ell} \varphi \mathcal{L}H_1 d\xi = [(H_0-1)(H_1''(\xi) - f'(H_0)H_1)$$
$$- H_1'(\xi)H_0'(\xi) + H_1 H_0''(\xi)]_{-\infty}^{\ell}. \qquad (15)$$

All contributions from the lower boundary vanish. On the upper boundary, H_1 follows from Eq. (2), where the asymptotic angle θ should be identified with the equilibrium contact angle, now set to unity. Otherwise, Eq. (2) retains the same form in rescaled coordinates. Comparing it to the derivative of Eq. (7),

$$[H'(\xi)]^3 = 1 + 3\delta \ln(\xi/\xi_0) = 1 + 3\delta H_1'(\xi), \qquad (16)$$

yields $H_1'(\xi) = \ln(\xi/\xi_0)$. Using this as well as $H_0(\ell) = \ell \gg 1$ in Eq. (15), we see that the two surviving contributions from the upper boundary are

$$-H_1'(\ell)H_0'(\ell) = -\ln(\ell/\xi_0) \quad \text{and} \quad H_1''H_0 = 1. \qquad (17)$$

The second integral in Eq. (14) is known as well from the static solution H_0. Passing from ξ to H_0 as the integration variable, this integral can be rewritten putting $d\xi = dH_0/H_0'(\xi) = y^{-1/2}dH_0$, where the function $y(H_0)$ is given by Eq. (9). The resulting integral diverges like $\ln \ell$ at $\ell \rightarrow \infty$. This divergence can be subtracted by presenting it in the form
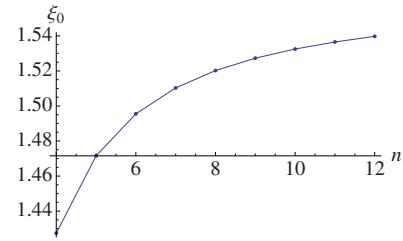

FIG. 2. (Color online) The dependence of the constant ξ_0 on n. The abscissa marks the analytical result for $n=5$.

$$\int_{-\infty}^{\ell} \frac{(H_0-1)^2}{H_0^3} d\xi = \int_1^{\ell}\left[\frac{(H_0-1)^2}{\sqrt{y}H_0^3} - \frac{1}{H_0}\right]dH_0 + \ln \ell. \qquad (18)$$

Combining Eqs. (17) and (18), we finally deduce that $1 - \ln \xi_0$ coincides with the limit $\ell \rightarrow \infty$ of the integral in Eq. (18):

$$\ln \xi_0 = \int_1^{\infty}\left[\frac{1}{H_0} - \left(1 - \frac{n-1}{n-3}\frac{1}{H_0^2}\right.\right.$$
$$\left.\left. + \frac{2}{n-3}\frac{1}{H_0^{n-1}}\right)^{-1/2}\frac{(H_0-1)^2}{H_0^3}\right]dH_0 - 1. \qquad (19)$$

The dependence of the constant ξ_0 on n is shown in Fig. 2. In the case $n=5$, we find analytically that $\xi_0 = 4/e$, in agreement with [10], for $n=7$, the result is

$$\xi_0(7) = \frac{\sqrt{6}+2}{4e(\sqrt{6}-2)^{\sqrt{8/3}}}. \qquad (20)$$

For most other values, the integral has to be computed numerically, but the dependence on n is rather weak.

Thus the constant ξ_0 is obtained without knowing H_1 inside the domain. It can be computed in this way for *any* suitable expression for disjoining pressure, up to a simple integration, which in some cases can be performed analytically. Once this constant is found, the intermediate solution can be now written in terms of the original variables as

$$[h'(x)]^3 = \theta_0^3 + 3\delta \ln\left(\frac{x\theta_0}{h_f \xi_0}\right). \qquad (21)$$

This expression can be matched to an appropriate outer solution in different macroscopic settings (see Sec. IV).

III. MATCHING TO A SPREADING DROP

Next we describe the matching between the intermediate region and a spreading drop. Again, Eq. (1) is to be solved perturbatively, expanding around the solution for a static drop. In the case without an external potential, which we are going to consider here, this is the solution of $\nabla^2 h_0 = \text{const}$. For a circular drop of volume V and radius R on a flat substrate, the solution is

$$h_0(r) = \frac{2V}{\pi R^2}\left[1 - \left(\frac{r}{R}\right)^2\right], \qquad (22)$$

where r is the radial coordinate. The drop meets the solid at

an *apparent* contact angle

$$\theta = \frac{4V}{\pi R^3}. \tag{23}$$

The static profile h_0 depends on time implicitly through its dependence on the drop radius R, cf. Eq. (22):

$$\frac{\partial h_0}{\partial t} = \dot{R} \frac{\partial h_0}{\partial R}. \tag{24}$$

Away from the contact line, all microscopic effects, such as disjoining pressure, can be neglected. We now introduce the expansion in the capillary number with U replaced by $\dot{R}$:

$$h_{out}(\mathbf{x}, t) = h_0(r) + \mathrm{Ca} h_1(\mathbf{x}) + O(\mathrm{Ca}^2). \tag{25}$$

The first-order equation obtained by expanding Eq. (1) has the general form (10) containing the linear operator

$$\mathcal{L} = \mathbf{\nabla} \cdot (h_0^3 \mathbf{\nabla} \nabla^2) \tag{26}$$

and the inhomogeneity

$$\psi(r) = -3 \frac{\partial h_0}{\partial R} = 3\theta \left[1 - 2 \left(\frac{r}{R} \right)^2 \right]. \tag{27}$$

The adjoint of $\mathcal{L}$ is

$$\mathcal{L}^\dagger = \nabla^2 [\mathbf{\nabla} \cdot (h_0^3 \mathbf{\nabla})]. \tag{28}$$

The symmetry leading to the existence of a zero eigenvalue of $\mathcal{L}$ and $\mathcal{L}^\dagger$ is now the reshaping symmetry changing the radius and the apparent contact angle at a constant volume, rather than the translational symmetry of the preceding section. The corresponding eigenfunction φ cannot be deduced directly from the zero-order solution as before, but computation of the solvability condition is made easier by making use of the volume conservation condition. Indeed, reducing the integral over the area A of the drop $\int \varphi \mathcal{L} h_1 d^2\mathbf{x}$ to a contour integral, it is sufficient to have a function $\varphi(\mathbf{x})$ satisfying $\mathcal{L}^\dagger \varphi = \mathrm{const}$ rather than $\mathcal{L}^\dagger \varphi = 0$, since the area integral (const $\int h_1 d^2\mathbf{x}$) remaining after integration by parts vanishes owing to volume conservation. This is ensured if φ is chosen such that

$$\mathbf{\nabla} \cdot (h_0^3 \mathbf{\nabla} \varphi) = h_0 + c. \tag{29}$$

An extra constant c is necessary since from Eq. (29)

$$\int_A (h_0 + c) d^2\mathbf{x} = \int_A \mathbf{\nabla} \cdot (h_0^3 \mathbf{\nabla} \phi) d^2\mathbf{x} = \int_{\partial A} h_0^3 (\mathbf{n} \cdot \mathbf{\nabla}) \phi = 0, \tag{30}$$

since $h_0 \to 0$ everywhere on the boundary ∂A. But the left-hand side of Eq. (30) is $V + Ac$, and thus $c = -V/A$; $\mathbf{n}$ is the normal to ∂A.

Multiplying Eq. (10) by the chosen eigenfunction and integrating over A yields, after four integrations by parts,

$$\int_A \varphi \psi d^2\mathbf{x} + \int_{\partial A} [\varphi h_0^3 \mathbf{n} \cdot \mathbf{\nabla} \nabla^2 h_1 - h_0^3 \mathbf{n} \cdot \mathbf{\nabla} \varphi \nabla^2 h_1$$
$$+ \mathbf{\nabla} \cdot (h_0^3 \mathbf{\nabla} \varphi) \mathbf{n} \cdot \mathbf{\nabla} h_1 - h_1 (\mathbf{n} \cdot \mathbf{\nabla}) \mathbf{\nabla} \cdot (h_0^3 \mathbf{\nabla} \varphi)] ds = 0. \tag{31}$$

This coordinate-free formulation is also applicable to more general situations involving an external potential (e.g., gravity) or a curved substrate.

Specifying to the simplest case of a drop on a flat substrate with gravity neglected, the function $\varphi(r)$ is calculated using Eqs. (22), (23), and (29) with $c = -V/A = -\theta R/4$ as

$$\varphi(r) = \int_0^r \frac{1}{r' h_0^3(r')} \int_0^{r'} r'' \left[h_0(r'') - \frac{\theta R}{4} \right] dr'' dr'$$
$$= \frac{r^2}{2\theta^2 (R^2 - r^2)}. \tag{32}$$

Since we expect $\int \psi \varphi r \, dr$ to diverge logarithmically matching Eq. (2), the integration in the solvability condition (31) cannot be extended to the contact line at $r = R$, but should be restricted to the interior of a circle $r < R - l$ with $l \ll 1$. Thus the solvability condition becomes

$$\int_0^{R-\ell} \varphi \psi r \, dr + \left\{ r \varphi h_0^3 \frac{d}{dr} \nabla^2 h_1 - r h_0^3 \varphi'(r) \nabla^2 h_1 \right.$$
$$\left. + h_1'(r) \frac{d}{dr} [r h_0^3 \varphi'(r)] - r h_1 \frac{d}{dr} \left[\frac{1}{r} \frac{d}{dr} [r h_0^3 \varphi'(r)] \right] \right\}_{r=R-\ell}$$
$$= 0. \tag{33}$$

The area integral is computed in the limit $\ell \to 0$ as

$$-3 \int_0^{R-\ell} \frac{\partial h_0}{\partial R} \varphi r \, dr \asymp \frac{3R^2}{4\theta} \left(\ln \frac{2\ell}{R} + 2 \right), \tag{34}$$

where $\asymp$ denotes an asymptotic value.

On the contour $r = R - \ell$, h_1 is obtained in the same way as in the preceding section by comparing the derivative of Eq. (25) with respect to r to the intermediate solution (2) where the asymptotic angle is identified with the apparent contact angle θ given by Eq. (23), which should be taken here with the negative sign:

$$[h'(r)]_{r=R-\ell}^3 = -\theta^3 + 9\mathrm{Ca} \ln(\ell/x_0) = -\theta^3 + 3\theta^2 \mathrm{Ca} h_1'(r), \tag{35}$$

leading to $h_1'(r) = 3\theta^{-2} \ln(\ell/x_0)$. Using also the asymptotic expressions for $\varphi \asymp R/(4\theta^2 \ell)$ and $h_0 \asymp \theta \ell$, we see that the last boundary term in Eq. (33) vanishes, while the first two cancel each other. The remaining term evaluates to

$$h_1'(r) \frac{d}{dr} [r h_0^3 \varphi'(r)] \asymp -\frac{3R^2}{4\theta} \ln \frac{\ell}{x_0}. \tag{36}$$

Adding Eqs. (34) and (36) up cancels the divergence, and we find finally

$$x_0 = R/(2e^2). \tag{37}$$

IV. EQUATION OF MOTION

We have presented above a simple method to calculate the free constant x_0 remaining in the universal viscous-capillary region near an advancing contact line by matching either to a macroscopic capillary profile or to the contact line region itself, avoiding explicit computation of perturbed solutions. It remains to reconcile the two results, which have to describe the same profile in the intermediate region $h_f \ll x \ll R$. This will lead us to the macroscopic equation of motion for the spreading droplet.

Absorbing now the equilibrium contact angle in the argument of the logarithm, we rewrite Eq. (21) as

$$[h'(x)]^3 = 9\text{Ca} \ln\left[\frac{\theta_0 x}{h_f \xi_0} \exp\left(\frac{\theta_0^3}{9\text{Ca}}\right)\right]. \quad (38)$$

In a similar way, Eq. (35) is rewritten using Eq. (37), replacing ℓ by x, and switching the sign of θ to yield

$$[h'(x)]^3 = 9\text{Ca} \ln\left[\frac{2e^2 x}{R} \exp\left(\frac{\theta^3}{9\text{Ca}}\right)\right]. \quad (39)$$

The two expressions have to coincide. This gives, after rearranging and replacing θ by the explicit expression (23), an equation of motion for the drop radius:

$$\left(\frac{4V}{\pi R^3}\right)^3 = \theta_0^3 + 9\dot{R}\frac{\eta}{\gamma}\ln\left(\frac{R\theta_0}{2e^2 h_f \xi_0}\right). \quad (40)$$

If the apparent angle θ is larger than θ_0, Eq. (40) describes the spreading of the drop until an equilibrium is reached at $\theta = \theta_0$. In the limit that θ is much larger than θ_0 initially, and neglecting the logarithmic dependence on R, one finds that $\dot{R} \propto R^{-9}$, and thus the time dependence $R \propto t^{1/10}$ know as Tanner's law [17].

Note, however, that it is *not* possible to simply put $\theta_0 = 0$ in order to describe the spreading of a perfectly wetting drop. As explained in [2], the argument of the logarithm in Eq. (38), which contains θ_0, acquires a nonanalytic time dependence on Ca. As a result, the matching can no longer be performed using an expansion in Ca, as we do here. Instead, one has to search for a similarity solution that contains Ca to the appropriate power. For a finite θ_0, the argument of the logarithm, containing the ratio of the macroscopic to the microscopic scale, is very large, but its influence is alleviated by a weak logarithmic dependence.

An alternative dimensionless form of Eq. (40), expressing the evolution of the apparent contact angle, is
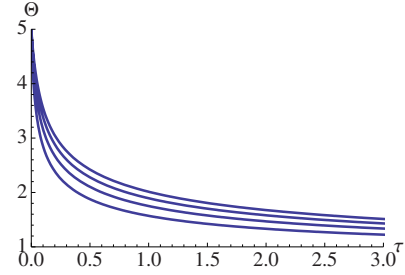

FIG. 3. (Color online) The dependence of the ratio of the apparent to the equilibrium contact angle Θ on the dimensionless time τ; the initial ratio is $\Theta(0) = 5$; log K changes from 15 (upper curve) to 6 (lower curve) with the increment 3.

$$\frac{d\Theta}{d\tau} = -\frac{\Theta^{4/3}(\Theta^3 - 1)}{\ln(K/\Theta)}, \quad (41)$$

where Θ is the ratio of the apparent to the equilibrium contact angle, τ is the dimensionless time variable, and K is a large parameter proportional to the ratio of the droplet volume to the cube of the microscopic length:

$$\Theta = \frac{\theta}{\theta_0}, \quad \tau = t\theta_0^3 \frac{\gamma}{\eta}\left(\frac{\pi\theta_0}{4V}\right)^{1/3}, \quad K = \frac{4V}{\pi}\frac{\theta_0^2}{(2e^2 h_f \xi_0)^3} \gg 1. \quad (42)$$

Some evolution curves $\Theta(\tau)$ are drawn in Fig. 3. The evolution is most sensitive to the logarithmic factor in the long-time limit. In this limit the deviation of the contact angle from its equilibrium value drops off like $\Theta - 1 \asymp \ln K^{1/3}/\tau$.

The structure of the equation of motion shows that the ratio of the capillary number to the cube of the slope, rather than the capillary number itself, is the true expansion parameter in the outer problem as well. Also note that Eq. (40) or Eq. (41) only represents one of the possible combinations between outer and inner solutions. Once the constant x_0 has been computed in a particular case, the equation of motion for any combination can be written down without any further calculation.

[1] L. M. Pismen, Colloids Surf., A **206**, 11 (2002).

[2] J. Eggers and H. A. Stone, J. Fluid Mech. **505**, 309 (2004).

[3] D. Bonn, J. Eggers, J. Indekeu, J. Meunier, and E. Rolley, Rev. Mod. Phys. (to be published).

[4] O. V. Voinov, Fluid Dyn. **11**, 714 (1976).

[5] L. M. Hocking, Q. Appl. Math. **36**, 55 (1983).

[6] J. Eggers, Phys. Fluids **17**, 082106 (2005).

[7] J. A. de Feijter, in *Thin Liquid Films*, edited by I. B. Ivanov (Marcel Dekker, New York, 1988), pp. 1–47.

[8] L. M. Pismen and Y. Pomeau, Phys. Rev. E **62**, 2480 (2000).

[9] L. M. Pismen, Phys. Rev. E **64**, 021603 (2001).

[10] J. Eggers, Phys. Rev. E **72**, 061605 (2005).

[11] L. M. Pismen and Y. Pomeau, Phys. Fluids **16**, 2604 (2004).

[12] L. M. Pismen, Phys. Rev. E **74**, 041605 (2006).

[13] B. V. Derjaguine, N. V. Churaev, and V. M. Muller, *Surface Forces* (Consultants Bureau, New York, 1987).

[14] S. Dietrich and M. Napiórkowski, Phys. Rev. A **43**, 1861

(1991).

[15] R. Seemann, S. Herminghaus, and K. Jacobs, J. Phys.: Condens. Matter **13**, 4925 (2001).

[16] R. Seemann (private communication).

[17] P.-G. de Gennes, Rev. Mod. Phys. **57**, 827 (1985).